Wiley Online Library
Early View publication on www.wileyonlinelibrary.com
(issue and page numbers not yet assigned;
citable using Digital Object Identifier – DOI)

Phys. Status Solidi RRL, 1–6 (2014) / DOI 10.1002/pssr.201409330

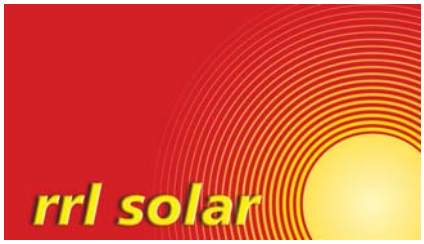

$CH_3NH_3PbI_3$/poly-3-hexylthiophen perovskite mesoscopic solar cells: Performance enhancement by Li-assisted hole conduction

Jin Hyuck Heo and Sang Hyuk Im*

Department of Chemical Engineering, Kyung Hee University, 1732 Deogyeong-daero, Giheung-gu, Yongin-si, Gyeonggi-do 446-701, Republic of Korea

Received 14 July 2014, revised 17 August 2014, accepted 21 August 2014
Published online 27 August 2014

Keywords $CH_3NH_3PbI_3$, perovskites, P3HT, electrical conduction, solar cells

* Corresponding author: e-mail imromy@khu.ac.kr

To address if the non-triphenylamine derivative hole transporting materials such as P3HT (poly-3-hexylthiophene) could also exhibit high device efficiency in mesoscopic $MAPbI_3$ perovskite solar cells, we examined the effect of Li-TFSI (Li-bis(trifluoromethanesulfonyl) imide) and t-BP (4-tert-butylpyridine) additives added in P3HT on device performance. Unlike the triphenylamine HTMs, the P3HT thiophene HTM without amine moiety was not doped by the additives but its conductivity was significantly improved by the Li-TFSI/t-BP mediated additional hole conduction. By inclusion of Li-TFSI/t-BP additive, we could fabricate more efficient mesoscopic $MAPbI_3$ perovskite solar cells with smaller hysteresis with respect to scan direction due to Li mediated additional hole conduction.

1 Introduction Solar energy has been considered as a promising alternative energy source among the renewable energy sources because it is clean, sustainable, and infinite. However, it is still required to reduce the power generation cost to compete the conventional fossil fuels. Therefore, it is still greatly challenging to develop much more cost-effective solar cells with high device efficiency and cheap manufacturing cost than the conventional crystalline Si solar cells. To develop solar cells satisfying these criteria, the second generation solar cells such as organic photovoltaics (OPVs), dye-sensitized solar cells (D-SSCs), and thin film solar cells (TFSCs) have been intensively studied to date.

As one effort to develop cost-effective solar cells, recently the solution processible solid-state perovskite hybrid solar cells with high efficiency have been reported and currently the power conversion efficiency reached over 16% at 1 sun condition [1]. Kojima et al. [2] first demonstrated the liquid type methylammonium lead triiodide/tribromide ($MAPbI_3$/$MAPbBr_3$) perovskite-sensitized solar cells and showed the possibility of new light absorbing materials in solar cells. Then Kim et al. [3] and Heo et al. [4] reported the solid state $MAPbI_3$ perovskite solar cells using Spiro-MeOTAD (2,2′,7,7′-tetrakis(N,N-di-p-methoxyphenylamine)-9,9′-spirobi-fluorene) and PTAA (poly triarylamine), respectively, as a hole transporting material (HTM) instead of liquid electrolyte. At the same time, Lee et al. [5] reported the mixed halide ($MAPbI_{3-x}Cl_x$) perovskite solar cells using Spiro-MeOTAD as HTM as well.

So far, intensive studies have been focused on the development of perovskite materials to control the bandgap by tuning the chemical composition of perovskite [6] or alloying the different perovskites [7]; and the development of new device architecture and process for the dense thin-film formation of perovskite through solution and vapor deposition methods [8]. Interesting is that most researchers use the triphenylamine moiety based HTMs such as Spiro-MeOTAD and PTAA with an exception for some researches. Recently, Abate et al. [9] reported that the oxidized Spiro-MeOTAD cations make complex with TFSI anions coming from Li-TFSI (Li-bis(trifluoromethanesulfonyl) imide) and consequently the doped Spiro-MeOTAD can exhibit improved hole conductivity.

Recently, it begins to be considered that the $MAPbI_3$ perovskite makes Wannier-type excitons (free charge charge carriers or weakly bound excitons) by illumination of light because its binding energy is $\sim 2k_BT$ (50 meV, where k_B is the Boltzmann constant and T the temperature) at ambient condition [10]. Therefore, we think that there will be no strict limit to choose HTMs as long as they transport the holes efficiently if we assume that their HOMO (highest occupied molecular orbital) or work function can be adjusted by chemical modification. Here, we choose the P3HT (poly-3-hexylthiophene) as a model HTM instead of triphenylamine based HTM and checked the effect of additives such as Li-TFSI and t-BP (4-tert-butylpyridine); which are known to enhance the hole mobility by forming complex with triphenylamine based HTMs; in order to demonstrate that the non-triphenylamine based HTMs can exhibit high device efficiency based on $MAPbI_3$ perovskite solar cells due to assisting of hole conduction by such additives.

2 Experimental

2.1 Preparation of $CH_3NH_3PbI_3$ perovskite solution CH_3NH_3I was synthesized by reacting 50 mL hydroiodic acid (57% in water, Aldrich) and 50 mL methylamine (40% in methanol, Junsei Chemical Co. Ltd.) in a 250-mL round-bottom flask at 0 °C for 2 h with stirring [1]. The precipitates were recovered by evaporation at 50 °C for 1 h. The products were dissolved in ethanol, recrystallized from diethyl ether, and finally dried at room temperature in a vacuum oven for 24 h. 40 wt% of $CH_3NH_3PbI_3$ solution was prepared by reacting the synthesized $CH_3NH_3I_3$ powder and PbI_2 (Aldrich) at 1 : 1 mole ratio in γ-butyrolactone at 60 °C for 30 min.

2.2 Device fabrication To prepare mesoscopic TiO_2 film, dense TiO_2 blocking layer (bl-TiO_2) of ca. 50 nm thickness was deposited on cleaned F-doped SnO_2 (FTO, Pilkington, TEC8) glass substrate by spray pyrolysis deposition (SPD) method with 20 mM of titanium diisopropoxide bis(acetylacetonate) (Aldrich) solution at 450 °C. To form 600 nm-thick mesoscopic TiO_2 film, TiO_2 paste (Dyesol DSL 18NR-T)/ethanol solution was spin coated on the bl-TiO_2/FTO substrate at 3000 rpm for 60 s and was then calcined at 450 °C for 1 h in air. To improve the interfacial contact between TiO_2 nanocrystals, the mesoscopic TiO_2 film was dipped into a 40 mM $TiCl_4$ aqueous solution for 12 h and washed with deionized water. The film was calcined again at 450 °C for 30 min. The 40 wt% $CH_3NH_3PbI_3$/γ-butyrolactone solution was then coated onto the mesoscopic TiO_2/bl-TiO_2/FTO substrate by spin-coating at 2000 rpm for 60 s then at 3000 rpm for 60 s and dried on a hot plate at 100 °C for 2 min. Poly-3-hexylthiophene (P3HT: Lumtec) hole transporting material was spin-coated on $CH_3NH_3PbI_3$/mesoscopic TiO_2/bl-TiO_2/FTO substrate at 3000 rpm for 30 s by using P3HT/toluene (15 mg/1 mL) with 7.5 μL Li-bis(trifluoromethanesulfonyl) imide (Li-TFSI)/acetonitrile (170 mg/1 mL) and 7.5 μL t-BP/acetonitrile (1 mL/1 mL) additives and without additives. Finally, Au counter electrode was deposited by thermal evaporation. The active area was fixed to 0.16 cm^2.

2.3 Device characterization The external quantum efficiency (EQE) was measured by a power source (ABET 150W xenon lamp, 13014) with a monochromator (DONGWOO OPTORN Co., Ltd., MonoRa-500i) and a potentiostat (IVIUM, IviumStat). The current density–voltage (J–V) curves were measured by a solar simulator (Peccell, PEC-L01) with a potentiostat (IVIUM, IviumStat) at 100 mA cm^{-2} illumination AM 1.5G and a calibrated Si-reference cell certificated by JIS (Japanese Industrial Standards). The J–V curves of all devices were measured by masking the active area with metal mask of 0.096 cm^2. The cyclic voltammetry (CV) of Li-TFSI solution (Li-TFSI/acetonitrile/toluene = 170 mg/1 mL/50 mL) was measured by a potentiostat (CH instruments, 600E) with conventional three-electrode system (reference electrode: Ag/AgCl, working electrode : Pt, counter electrode : Pt) at 50 mV of scan rate. For the measurement of hole conductivity P3HT and P3HT/additives, the P3HT/toluene (15 mg/1mL) with Li-TFSI/t-BP additives and without additives was spin-coated on bl-TiO_2/FTO substrate at 2000 rpm for 30 s and Au counter electrode was deposited by thermal evaporator. The active area of both devices was fixed to 0.16 cm^2 and current–voltage (I–V) curves were measured at dark state.

3 Results and discussion We conceive that Li-TFSI/t-BP additives will act as a redox shuttle of Li/Li^+ because Li-TFSI is good electrolyte for secondary Li-ion battery. Therefore, we depicted our schematic concept for the operation mechanism of $MAPbI_3$ perovskite solar cell with P3HT HTM containing Li-TFSI/t-BP additives as shown in Fig. 1. Upon illumination of light, the electron–hole pairs are generated by $MAPbI_3$ sensitizer and the electrons (holes) are transported into mesoscopic TiO_2 electron conductor (P3HT HTM containing additives). In the mesoscopic $MAPbI_3$ perovskite solar cell, the pores of mesoscopic TiO_2 are mostly infiltrated by $MAPbI_3$ perovskite and thin overlayers of perovskite are formed on top of the mesoscopic TiO_2 electrode, whereas most HTM is covered on the perovskite layer/mesoscopic TiO_2. Therefore, the generated electrons can be easily injected into adjacent mesoscopic TiO_2 electrode of ~600 nm thickness but the holes will not effectively extracted out to the HTM far from the $MAPbI_3$/mesoscopic TiO_2 electrode because the diffusion length of electrons and holes is ~100 nm [11]. Accordingly it is expected that the device efficiency will be degraded if the HTM could not effectively transport the holes from the $MAPbI_3$ perovskite layer because the flux of electrons will be larger than that of holes owing to the larger interfacial area between perovskite and mesoscopic TiO_2 than the perovskite/HTM interfacial area. Namely, the hole conductivity of HTM will determine the overall device performance and we conceive that the Li-TFSI/t-BP

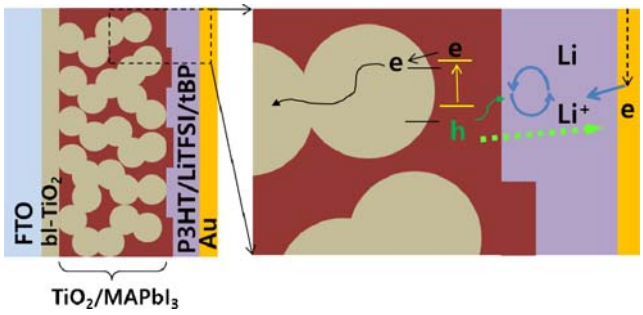

Figure 1 Schematic illustration of mesoscopic $MAPbI_3$ perovskite solar cell's device operation by Li-assisted hole conduction.

additives will assist additional hole conduction-like quasi-solid electrolyte leading enhancement of overall device performance as illustrated in Fig. 1.

To check if the additives can enhance the device performance, we compared photocurrent density–voltage (J–V) curves of FTO/bl-TiO_2/mesoscopic TiO_2/$MAPbI_3$ perovskite/P3HT solar cells with and without Li-TFSI/t-BP additives with respect to scan direction as shown in Fig. 2(a). The deviation of efficiency of mesoscopic $MAPbI_3$/P3HT hybrid solar cells with and without additives is also shown in Fig. S1 (see Supporting Information). The J–V curves of mesoscopic $MAPbI_3$/P3HT solar cells with and without additives exhibited hysteresis with respect to scan direction possibly due to charge accumulation in $MAPbI_3$ perovskite. However, the mesoscopic $MAPbI_3$/P3HT solar cells with additive show smaller hysteresis of J–V curves than that without additive. This might be attributed to the better charge transport in $MAPbI_3$/P3HT solar cells with additive due to the enhanced conductivity by additives. The average device performance of mesoscopic $MAPbI_3$ perovskite solar cell with additives was greatly enhanced as shown in Fig. S1. The best $MAPbI_3$/P3HT hybrid solar cells with and without additives measured by forward scan direction had short-circuit current density (J_{sc} = 20.1 mA/cm^2), open-circuit voltage (V_{oc} = 0.92 V), fill factor (FF = 74%) and overall power conversion efficiency (η = 13.7%) at 1 sun condition, whereas the solar cell without additives exhibited poor efficiency (J_{sc} = 15.5 mA/cm^2, V_{oc} = 0.67 V, FF = 55%, and η = 5.7%) the value of which is consistent with the previously reported Ref. [4]. Here it is noted that the $MAPbI_3$/P3HT solar cells with additives show smaller hysteresis of efficiency under forward (η = 13.7%) and backward (η = 14.2%) scan direction than those without additives (forward: 5.7%, backward: 6.5%). The external quantum efficiency (EQE) spectra of mesoscopic $MAPbI_3$ perovskite solar cells with and without additives in Fig. 2(b) indicate that the charge transfer and charge collection efficiency is greatly enhanced by introduction of Li-TFSI and t-BP in P3HT HTM because the absorption spectra of each sample were similar. The dimple around 650 nm wavelength in EQE spectra is attributed to absorption of P3HT HTM because the electron–hole pairs generated by the light absorption of P3HT are not likely to be effectively transferred to mesoscopic TiO_2/$MAPbI_3$ perovskite.

In order to investigate the role of additives on device performance, we fabricated mesoscopic $MAPbI_3$ perovskite solar cells with P3HT HTM containing only Li-TFSI and only t-BP additive, respectively, and checked their device efficiencies as shown in Fig. 3. To check the effect of Li-TFSI on device performance, we added 5, 10, and 15 µL of Li-TFSI/acetonitrile (ACN) solution (170 mg/1 mL) in 1 mL of P3HT/toluene solution (15 mg/1 mL) and formed the P3HT/Li-TFSI hole transporting layer by spin-coating. Here the Li-TFSI/ACN solution was used because Li-TFSI itself is insoluble to P3HT/toluene solution but small amount of ACN co-solvent enables Li-TFSI to be dissolved in P3HT/toluene solution. Figure 3(a) exhibited that the device efficiency is fluctuated with concentration of Li-TFSI which might be attributed to the formation of solid Li-TFSI within P3HT hole transporting layer because the Li-TFSI is re-precipitated within P3HT layer by solvent evaporation (ACN and toluene) during spin-coating process so that the solid Li-TFSI precipitate causes the formation of pin-

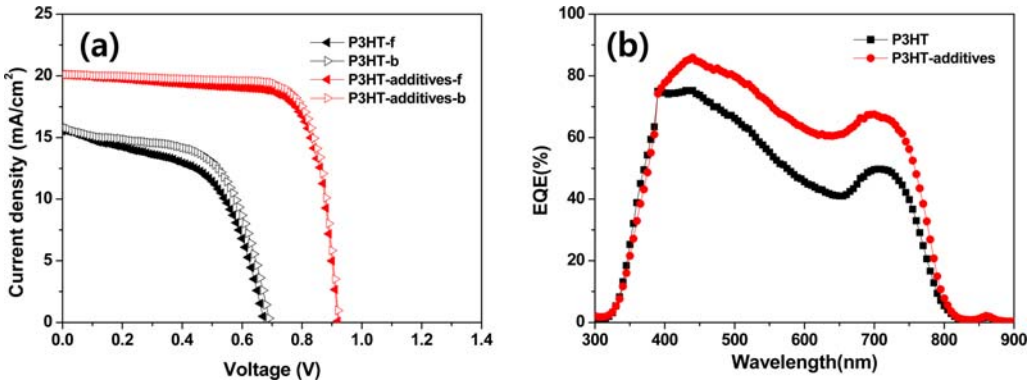

Figure 2 (a) Current density–voltage (J–V) curves of mesoscopic $MAPbI_3$/P3HT solar cells with and without Li-TFSI/t-BP additives with respect to forward and backward scan direction (f = forward, b = backward, delay time = 200 ms) and (b) their external quantum efficiency (EQE). 15 µL of Li-TFSI/ACN (170 mg/1 mL) and 15 µL of t-BP/ACN (1 mL/1 mL) additives are added in 1 mL of P3HT/toluene solution (15 mg/1 mL).

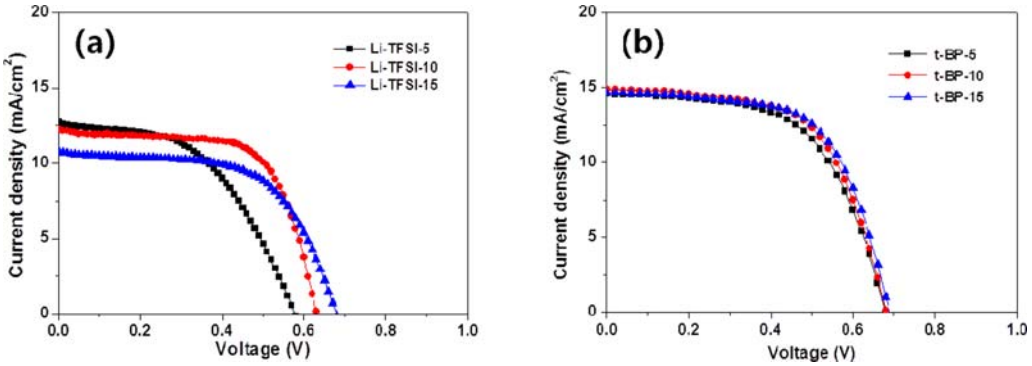

Figure 3 Effect of Li-TFSI and t-BP additives on device performance. $J-V$ characteristics with the concentration variation of (a) Li-TFSI and (b) t-BP added in P3HT hole transporting layer of mesoscopic $MAPbI_3$ perovskite solar cell. Additive-x: x denotes x μL of Li-TFSI/ACN (170 mg/1 mL) or t-BP/ACN (1 mL/1 mL) additive mixed in 1 mL of P3HT/toluene solution (15 mg/1 mL).

holes in P3HT layer. The pinholes lead Au counter electrode to be directly contacted with mesoscopic TiO_2 or $MAPbI_3$ layer, which increases the backward recombination. Accordingly the device efficiency is dependent on the morphology of P3HT + Li-TFSI layer causing significant deviation of device performance. On the other hand, Fig. 3(b) shows that the t-BP additive does not affect the device efficiency because the small amount of liquid residual t-BP in P3HT film after spin-coating process will not significantly degrade the device efficiency. Here we conclude that the device performance is greatly enhanced only when both of Li-TFSI and t-BP additives are present in P3HT HTM. The boiling temperature of ACN, toluene, and t-BP is 82, 110, and 196 °C, respectively, so that t-BP can be remained in P3HT HTM after spin-coating whereas ACN and toluene will be completely dried. This implies that the P3HT HTM does not make complex with Li-TFSI/t-BP additives unlike triphenyl amine based HTMs.

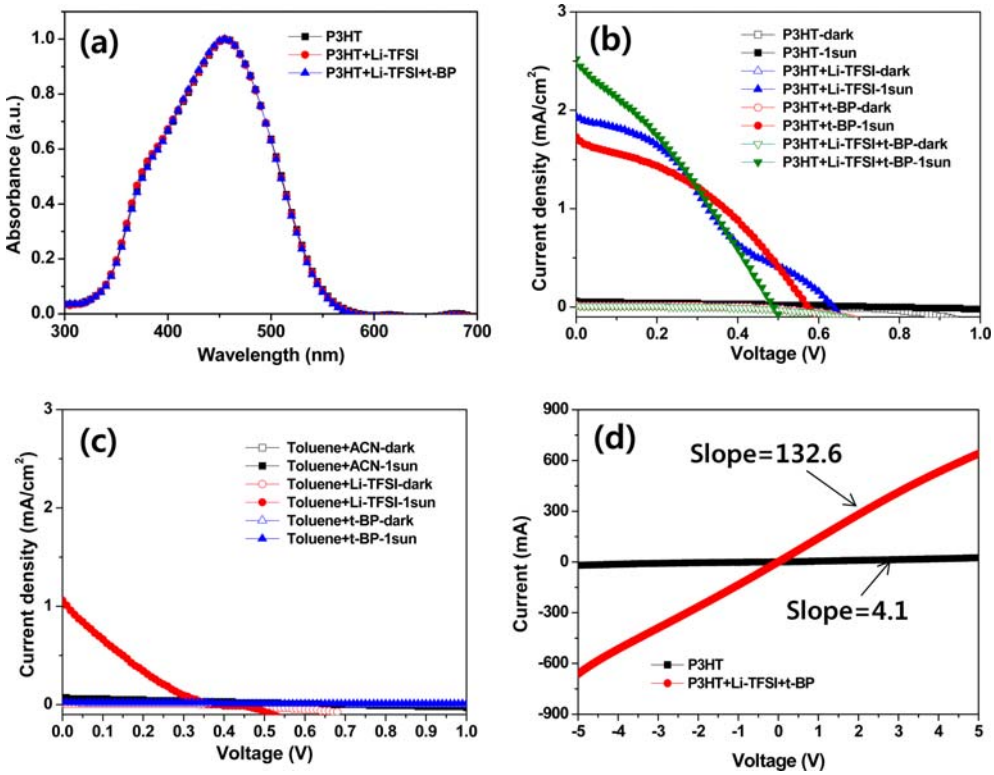

Figure 4 (a) UV-visible absorption spectra of P3HT, P3HT + Li-TFSI, and P3HT + Li-TFSI + t-BP in 50 mL-toluene solution: P3HT = 100 μL of P3HT/toluene (15 mg/1 mL), Li-TFSI = 100 μL of Li-TFSI/ACN (170 mg/1 mL), and t-BP = 100 μL of t-BP/ACN (1 mL/1 mL); current density–voltage ($J-V$) curves of liquid junction mesoscopic $MAPbI_3$ solar cells, (b) with and (c) without P3HT in FTO/bl-TiO_2/mesoscopic TiO_2/$MAPbI_3$/P3HT + (additives) + toluene solution/FTO; and (d) current–voltage ($I-V$) curves of P3HT film with and without additives.

Table 1 Summary of device performance in mesoscopic $MAPbI_3$ perovskite solar cells with and without Li-TFSI/t-BP additives in P3HT hole transporting layer.

		V_{oc} (V)	J_{sc} (mA/cm^2)	FF (%)	η (%)
P3HT	forward	0.67	15.5	55	5.7
	backward	0.69	15.8	60	6.5
P3HT-additives	forward	0.92	20.1	74	13.7
	backward	0.92	20.1	77	14.2

To understand the role of Li-TFSI/t-BP additives in P3HT HTM, first we checked the UV-Visible spectra of P3HT, P3HT + Li-TFSI, and P3HT + Li-TFSI + t-BP solution with small amount of ACN as shown in Fig. 4(a) because if the additives make certain complex form with P3HT, the solution will make additional absorption spectra. However, all of the three absorption spectra were exactly matched and additional absorption peaks do not appear. Therefore we could exclude the effect of complex form between P3HT and additives. Secondly, we checked if the Li-TFSI/t-BP additives act as redox shuttle by measuring J–V characteristics of liquid junction mesoscopic $MAPbI_3$ solar cells comprised with FTO/bl-TiO_2/mesoscopic TiO_2/$MAPbI_3$/P3HT + (additives) + toluene solution/FTO as shown in Fig. 4(b). The device with P3HT + toluene (concentration = 15 mg/1 mL in P3HT/toluene) solution as electrolyte does not show any response to light illumination and consequently the J_{sc} value of the cell under illumination of 1 sun was almost identical to the dark state. On the other hand, the devices with P3HT + Li-TFSI + toluene, P3HT + t-BP + toluene, and P3HT + Li-TFSI + t-BP + toluene solution as electrolyte exhibited J_{sc} of 2.0, 1.75, and 2.5 mA/cm^2 at 1 sun condition, respectively. It is quite interesting that all of the three liquid junction $MAPbI_3$ perovskite solar cells with P3HT solutions containing additives showed photoresponse under illumination of 1 sun meanwhile the solid mesoscopic $MAPbI_3$ perovskite solar cell with P3HT HTM containing both Li-TFSI and t-BP additives had only great enhancement of device efficiency. It is attributed to non-solvent effect of t-BP in P3HT + toluene solution because upon adding 15 µL of t-BP/CAN (1/1 v/v) into 1 mL of P3HT + toluene solution, the red-orange color of P3HT + toluene solution is changed to dark purple solution whereas the others are not, which indicates that the P3HT is precipitated (recrystallized) from the parent solution. It is also considered that here we added 15 µL of ACN in 1 mL P3HT + toluene solution for pre-dissolution of Li-TFSI. To verify what enables photoresponse of $MAPbI_3$ perovskite solar cell among ACN, Li-TFSI, and t-BP, we fabricated liquid junction $MAPbI_3$ solar cells without P3HT as shown in Fig. 4(c). This clearly confirms that the Li-TFSI solely acts as redox shuttle among them. The cyclic voltamogram (CV) of Li-TFSI/ACN (170 mg/1 mL) in toluene (50 mL) solvent in Fig. S2 also confirms that the Li-TFSI can act as redox shuttle whereas the others such as t-BP/toluene and ACN/toluene did not show any reduction and oxidation peaks. Finally, we measured conductivity of P3HT film with and without additives by fabricating ITO/P3HT/Au. The I–V curves of P3HT film with and without additive were shown in Fig. 4(d). The DC (direct current) conductivity (σ_0) can be determined from the slope of I–V plot, $I = \sigma_0(A/d)\,V$, where A is the area of the sample (0.16 cm^2) and d is the thickness of the sample (20 µm), respectively [12] The calculated conductivities of P3HT with and without additives are 1.6×10^{-3} and 5.0×10^{-5} S/cm. The calculated conductivity of P3HT without additives was consistent with the reported conductivity (6.675×10^{-5} S/cm) [13]. This clearly confirms that the conductivity of P3HT is ~32-fold increased by addition of Li-TFSI and t-BP additives. From the above experimental results, we could conclude that the great enhancement of mesoscopic $MAPbI_3$ perovskite solar cells with P3HT + Li-TFSI/t-BP additives is attributed to the improved hole conductivity due to the Li mediated additional hole conduction by the role as redox shuttle of Li-TFSI/t-BP.

4 Conclusion In summary, we successfully demonstrated that the P3HT HTM with Li-TFSI/t-BP additives as a model HTM of non-triphenylamine derivative ones could exhibit high device performance in mesoscopic $MAPbI_3$ perovskite solar cells due to Li-TFSI/t-BP mediated additional hole conduction. Unlike the triphenylamine HTMs, the P3HT thiophene HTM without amine moiety is not doped by the additives because it does not make a complex form with TFSI anion. On the other hand, we elucidated that the Li-TFSI/t-BP additives in P3HT HTM can transport the holes generated by $MAPbI_3$ perovskite to a counter Au electrode as like to the redox shuttle in liquid/gel electrolyte. Therefore, the P3HT with Li-TFSI/t-BP additives showed better hole conductivity than the P3HT without additives due to the additional hole transport by Li-TFSI/t-BP mediated hole conduction. By introduction of Li-TFSI/t-BP additives in P3HT HTM, we could greatly enhance the device efficiency from 6.5% to 13.5% at 1 sun condition. We believe that non-triphenylamine derivative HTMs will also be applicable to attain high device efficiency in mesoscopic $MAPbI_3$ perovskite solar cells by controlling HOMO (highest occupied molecular orbital), hole mobility/conductivity, and formulating with additives.

Supporting Information Supporting Information is available from Wiley Online Library or from the author.

Acknowledgements This study was supported by Mid-career Research Program (No. NRF-2013R1A2A2A01067999) and by Basic Science Research Program (No. 2014R1A5A1009799) through the National Research Foundation of Korea (NRF) funded by the Ministry of Science, ICT & Future Planning.

References

[1] N. J. Jeon, H. G. Lee, Y. C. Kim, J. Seo, J. H. Noh, J. Lee, and S. I. Seok, J. Am. Chem. Soc. **136**, 7837 (2014).

[2] A. Kojima, K. Teshima, Y. Shirai, and T. Miyazaka, J. Am. Chem. Soc. **131**, 6050 (2009).
[3] H.-S. Kim, C.-R. Lee, J.-H. Im, K. B. Lee, T. Moehl, S.-J. Moon, R. Humphry-Baker, J.-H. Yum, J. E. Moser, M. Grätzel, and N. G. Park, Sci. Rep. **2**, 591 (2012).
[4] J. H. Heo, S. H. Im, J. H. Noh, T. N. Mandal, C. S. Lim, J. A. Chang, Y. H. Lee, H.-J. Kim, A. Sarkar, M. K. Nazeeruddin, M. Grätzel, and S. I. Seok, Nature Photon. **7**, 486 (2013).
[5] M. M. Lee, J. Teuscher, T. Miyasaka, T. N. Murakami, and H. J. Snaith, Science **338**, 643 (2012).
[6] J. H. Noh, S. H. Im, J. H. Heo, T. N. Mandal, and S. I. Seok, Nano Lett. **13**, 1764 (2013).
[7] Y. Ogomi, A. Morita, S. Tsukamoto, T. Saitho, N. Fujikawa, Q. Shen, T. Toyoda, K. Yoshino, S. S. Pandey, T. Ma, and S. Hayase, J. Phys. Chem. Lett. **5**, 1004 (2014).
[8] M. Liu, M. B. Johnston, and H. J. Snaith, Nature **501**, 395 (2013).
[9] A. Abate, T. Leijtens, S. Pathak, J. Tescher, R. Avolio, M. E. Errico, J. Kirkpatrik, J. M. Ball, P. Docampo, I. McPherson, and H. J. Snaith, Phys. Chem. Chem. Phys. **15**, 2572 (2013).
[10] S. D. Stranks, G. E. Eperon, G. Grancini, C. Menelaou, M. J. P. Alcocer, T. Leijtens, L. M. Herz, A. Petrozza, and H. J. Snaith, Science **342**, 341 (2013).
[11] G. Xing, N. Mathews, S. Sun, S. S. Lim, Y. M. Lam, M. Grätzel, S. Mhaislkar, and T. C. Sum, Science **342**, 344 (2013).
[12] J. Obrzut and K. A. Page, Phys. Rev. B **80**, 195211 (2009).
[13] B. K. Kulla and A. K. Nandi, Macromolecules **37**, 8577 (2004).